

A Novel Approach to Model Hybrid Stars

V.A. Dexheimer*

FIAS, Johann Wolfgang Goethe University, Frankfurt am Main, Germany

S. Schramm†

CSC, FIAS, ITP, Johann Wolfgang Goethe University, Frankfurt am Main, Germany

(Dated: October 25, 2018)

We extend the hadronic SU(3) non-linear sigma model to include quark degrees of freedom. The choice of potential for the deconfinement order parameter as a function of temperature and chemical potential allows us to construct a realistic phase diagram from the analysis of the order parameters of the system. These parameters are the chiral condensate, for the chiral symmetry restoration, and the scalar field Φ (as an effective field related to the Polyakov loop) for the deconfinement to quark matter. Besides reproducing lattice QCD results, for zero and low chemical potential, we are in agreement with neutron star observations for zero temperature.

PACS numbers:

The models used to describe neutron stars can generally be divided into two classes. The first class includes approaches in which the constituent particles are hadrons [1–3]. Some of them incorporate certain symmetries from QCD, like chiral symmetry, but they do not include deconfinement. Examples of these are hadronic sigma models [4–7]. The second class includes quark star models, which usually do not directly incorporate hadronic degrees of freedom in the model formulation. Examples of these are bag-model studies [8] as well as quark-NJL model and quark sigma-models [9].

Using these approaches hybrid neutron stars, which consist of a hadronic and a quark phase, are normally described by adopting two different models with separate equations of state for hadronic and quark matter (see e.g. [10]). They are connected at the chemical potential in which the pressure of the quark EOS exceeds the hadronic one, signalling the phase transition to quark matter. Within our approach we employ a single model for the hadronic and for the quark phase.

The extension of the hadronic SU(3) non-linear sigma model to quark degrees of freedom is constructed in a spirit similar to the PNJL model [11], in the sense that it is a non-linear sigma model that introduces a scalar field which suppresses the quark degrees of freedom at low densities/temperatures. In QCD this scalar field was named Polyakov loop and is defined via $\Phi = \frac{1}{3}\text{Tr}[\exp(i \int d\tau A_4)]$, where $A_4 = iA_0$ is the temporal component of the SU(3) gauge field. In our case, this scalar field is also called Φ , in analogy to the PNJL approach with an effective potential for the field, as discussed below, that drives the phase transition in the field Φ representing a phenomenological description of the transition from the confined to the deconfined phase.

The Lagrangian density of the non-linear sigma model

in mean field approximation reads:

$$L = L_{Kin} + L_{Int} + L_{Self} + L_{SB} - U, \quad (1)$$

where besides the kinetic energy term for hadrons, quarks, and leptons (included to insure charge neutrality) the terms:

$$L_{Int} = -\sum_i \bar{\psi}_i [\gamma_0 (g_{i\omega}\omega + g_{i\phi}\phi + g_{i\rho}\tau_3\rho) + M_i^*] \psi_i, \quad (2)$$

$$\begin{aligned} L_{Self} = & -\frac{1}{2}(m_\omega^2\omega^2 + m_\rho^2\rho^2 + m_\phi^2\phi^2) \\ & +g_4\left(\omega^4 + \frac{\phi^4}{4} + 3\omega^2\phi^2 + \frac{4\omega^3\phi}{\sqrt{2}} + \frac{2\omega\phi^3}{\sqrt{2}}\right) \\ & +k_0(\sigma^2 + \zeta^2 + \delta^2) + k_1(\sigma^2 + \zeta^2 + \delta^2)^2 \\ & +k_2\left(\frac{\sigma^4}{2} + \frac{\delta^4}{2} + 3\sigma^2\delta^2 + \zeta^4\right) + k_3(\sigma^2 - \delta^2)\zeta \\ & +k_4 \ln \frac{(\sigma^2 - \delta^2)\zeta}{\sigma_0^2\zeta_0}, \end{aligned} \quad (3)$$

$$L_{SB} = m_\pi^2 f_\pi \sigma + \left(\sqrt{2}m_k^2 f_k - \frac{1}{\sqrt{2}}m_\pi^2 f_\pi\right) \zeta, \quad (4)$$

represent the interactions between baryons (and quarks) and vector and scalar mesons, the self interactions of scalar and vector mesons and an explicit chiral symmetry breaking term, responsible for producing the masses of the pseudo-scalar mesons. The Φ potential U will be discussed in the following. The underlying flavor symmetry of the model is SU(3) and the index i denotes the baryon octet and the three light quarks. The mesons included are the vector-isoscalars ω and ϕ , the vector-isovector ρ , the scalar-isoscalars σ and ζ (strange quark-antiquark state) and the scalar-isovector δ . The isovector mesons affect isospin-asymmetric matter and are consequently important for neutron star physics. The coupling constants of the model are shown in Table. I. They were fitted to reproduce the vacuum masses of the baryons and mesons, nuclear saturation properties (density $\rho_0 = 0.15$

*Electronic address: dexheimer@th.physik.uni-frankfurt.de

†Electronic address: schramm@th.physik.uni-frankfurt.de

TABLE I: Coupling constants for the model containing only baryons

$g_{N\omega} = 11.90$	$g_{N\phi} = 0$	$g_{N\rho} = 4.03$
$g_{N\sigma} = -9.83$	$g_{N\delta} = -2.34$	$g_{N\zeta} = 1.22$
$g_{\Lambda\omega} = 7.93$	$g_{\Lambda\phi} = -7.32$	$g_{\Lambda\rho} = 0$
$g_{\Lambda\sigma} = -5.52$	$g_{\Lambda\delta} = 0$	$g_{\Lambda\zeta} = -2.30$
$k_0 = 1.19$	$k_1 = -1.40$	$k_2 = 5.55$
$k_3 = 2.65$	$k_4 = -0.06$	$g_4 = 38.9$

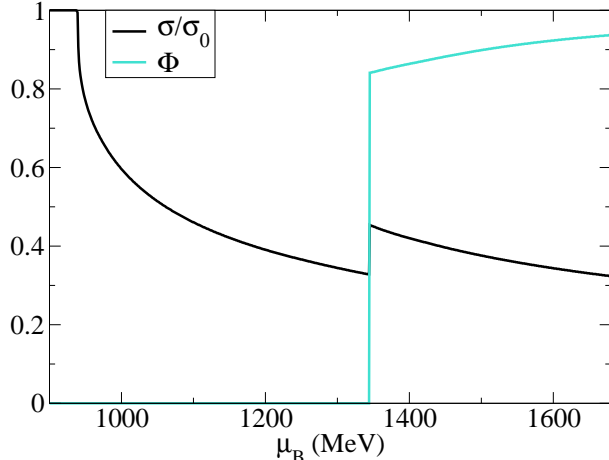


FIG. 1: (Color online) Order parameters for chiral symmetry restoration and deconfinement to quark matter as a function of baryonic chemical potential for star matter at zero temperature.

fm⁻³, binding energy per nucleon $B/A = -16.00$ MeV, nucleon effective mass $M_N^* = 0.67 M_N$, compressibility $K = 297.32$ MeV), asymmetry energy ($E_{sym} = 32.50$ MeV), and reasonable values for the hyperon potentials ($U_\Lambda = -28.00$ MeV, $U_\Sigma = 5.35$ MeV, $U_\Xi = -18.36$ MeV). The vacuum expectation values of the scalar mesons are constrained by reproducing the pion and kaon decay constants. A detailed discussion of the purely hadronic part of the Lagrangian can be found in [4, 12, 13].

The mesons are treated as classical fields within the mean-field approximation [14]. Finite-temperature calculations include the heat bath of hadronic and quark quasiparticles within the grand canonical potential of the system. It is defined as:

$$\frac{\Omega}{V} = -L_{Int} - L_{Self} - L_{SB} - L_{Vac} \\ \mp T \sum_i \frac{\gamma_i}{(2\pi)^3} \int_0^{k_{F_i}} d^3k \ln(1 \pm e^{-\frac{1}{T}(E_i^*(k) - \mu_i^*)}), \quad (5)$$

where L_{Vac} is the vacuum energy, γ_i the fermionic degeneracy, $E_i^*(k) = \sqrt{k^2 + M_i^{*2}}$ the single particle effective energy, and $\mu_i^* = \mu_i - g_{i\omega}\omega - g_{i\phi}\phi - g_{i\rho}\tau_3\rho$ the effective chemical potential of each species. The chemical potential for each species μ_i comes from the chemical equilib-

rium conditions. Finite temperature calculations also include a gas of free pions and kaons. As they have very low mass, they dominate the low density/ high temperature regime. All calculations were performed considering zero net strangeness except the zero temperature star matter case since, for neutron stars, the time scale is large enough for strangeness not to be conserved.

The effective masses of the baryons and quarks are generated by the scalar mesons except for a small explicit mass term M_0 (equal to 150 MeV for nucleons, 354 MeV for hyperons, 5 MeV for up and down quarks and 150 MeV for strange quarks) and the term containing Φ :

$$M_B^* = g_{B\sigma}\sigma + g_{B\delta}\tau_3\delta + g_{B\zeta}\zeta + M_{0_B} + g_{B\Phi}\Phi^2, \quad (6)$$

$$M_q^* = g_{q\sigma}\sigma + g_{q\delta}\tau_3\delta + g_{q\zeta}\zeta + M_{0_q} + g_{q\Phi}(1 - \Phi). \quad (7)$$

With the increase of temperature/density, the σ field (non-strange chiral condensate) decreases its value, causing the effective masses of the particles to decrease towards chiral symmetry restoration. The field Φ assumes non-zero values with the increase of temperature/density and, due to its presence in the baryons effective mass (Eq. (6)), suppresses their presence. On the other hand, the presence of the Φ field in the effective mass of the quarks, included with a negative sign (Eq. (7)), insures that they will not be present at low temperatures/densities. As can be seen from the different orders of Φ and different signs in the new effective mass terms, the motivation for this construction is not derived from QCD. It is a simple effective way to change degrees of freedom within the same model. Note that in the PNJL approach the coupling of the quarks to the Polyakov loop can be derived to be included in the quark and antiquark distribution functions in the grand canonical potential. However, this leads to non-vanishing quasi-quark contributions at any temperature below T_c , which we avoid in our phenomenological approach (Eqs. (6,7)).

The behavior of the order parameters of the model is shown in Fig. 1 for neutron star matter at zero temperature. The difference between this kind of matter and the so-called symmetric matter comes from the assumption of charge neutrality, essential for the stability of neutron stars, and beta equilibrium. In this case, the chiral symmetry restoration, which is a crossover for purely hadronic matter, turns into a first order phase transition by the influence of the strong first order transition to deconfined matter. The model is consistent in the sense that both order parameters are related. The small increase in the chiral condensate value during the transition is due to the smaller quark baryon number (1/3) compared to the baryonic one.

The effective normalized masses of baryons and quarks show the relation between these quantities and the order parameters, responsible for the dynamics of the model (Fig. 1 and 2). Since the coupling constants in the Φ term of the effective mass formulas are high but still finite, the effective masses of the degrees of freedom not

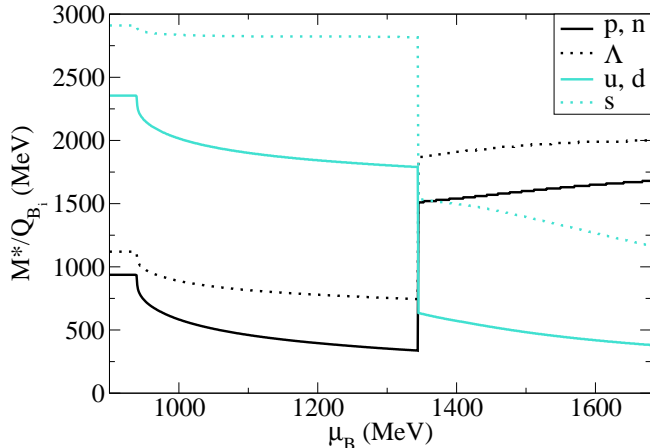


FIG. 2: (Color online) Effective normalized mass of different species as a function of baryonic chemical potential for star matter at zero temperature.

TABLE II: Additional coupling constants for the model containing baryons and quarks

$g_{q\omega} = 0$	$g_{q\phi} = 0$	$g_{q\rho} = 0$
$g_{q\sigma} = -3.00$	$g_{q\delta} = 0$	$g_{q\zeta} = -3.00$
$a_0 = -1.85$	$a_1 = -1.44 \times 10^{-3}$	$a_2 = -0.08$
$a_3 = -0.40$	$g_{B\Phi} = 1500 \text{ MeV}$	$g_{q\Phi} = 500 \text{ MeV}$
$T_0 = 200 \text{ MeV}$	$T_0 = 270 \text{ MeV}$ for pure gauge case	

effectively present in each phases are high but also finite. The effective masses normalized by the baryonic number are shown in Fig. 2. These quantities are directly related to the onset of particles appearance in the system, that reads:

$$\mu_{B_{onset}} = \frac{M_i^*}{Q_{B_i}} + \mu_e \frac{Q_i}{Q_{B_i}} - \mu_S \frac{Q_{S_i}}{Q_{B_i}} + \frac{g_{i\omega}\omega + g_{i\phi}\phi + g_{i\rho}\tau_3\rho}{Q_{B_i}}, \quad (8)$$

where Q_{B_i} is the baryonic number, μ_e is the electron chemical potential, Q_i is the electric charge, μ_S the strange chemical potential, and Q_{S_i} the strangeness of each species.

Continuing the analogy to the PNJL model, the potential U for Φ reads:

$$U = (a_0 T^4 + a_1 \mu^4 + a_2 T^2 \mu^2) \Phi^2 + a_3 T_0^4 \log(1 - 6\Phi^2 + 8\Phi^3 - 3\Phi^4). \quad (9)$$

It is a simplified version of the potential used in [15, 16] and adapted to also include terms that depend on the chemical potential. The two extra terms (that depend on the chemical potential) are not unique, but the most simple natural choice whose parameters are chosen to reproduce the main features of the phase diagram at finite

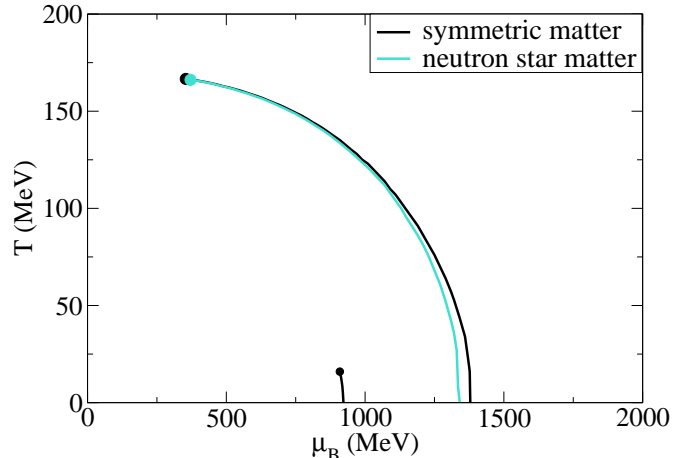


FIG. 3: (Color online) Phase diagram: temperature versus baryonic chemical potential. The lines represent first order transitions. The circles mark the critical end-points.

densities. While in the first part of the potential Φ^2 ensures U to be bound from below, in the second part of the potential $T_0^4 \log(1 - 6\Phi^2 + 8\Phi^3 - 3\Phi^4)$ ensures that Φ is always (for any region of the phase diagram) bound between zero and one.

The coupling constants for the quarks are shown in Tab. II and are chosen to reproduce lattice data as well as known information about the phase diagram. The lattice data includes a first order phase transition at $T = 270 \text{ MeV}$ and a pressure functional $P(T)$ similar to Refs. [15, 16] at $\mu = 0$ for pure gauge, a crossover at vanishing chemical potential with a transition temperature of 171 MeV (determined as the peak of the change of the chiral condensate and Φ) and the location of the critical end-point (at $\mu_c = 354 \text{ MeV}$, $T_c = 167 \text{ MeV}$ for symmetric matter in accordance with one of the existent calculations [17]). The phase diagram information includes a continuous first order phase transition line that terminates on the zero temperature axis at four times saturation density.

As can be seen in Fig. 3, the transition from hadronic to quark matter obtained is a crossover for small chemical potentials. Beyond the critical end-points a first order transition lines for symmetric as well as for star matter begin. The critical temperatures for chiral symmetry restoration coincide with the ones for deconfinement in both cases. Since the model is able to reproduce nuclear matter saturation at realistic values for the saturation density, nuclear binding energy, as well as the compressibility and asymmetry energy, we also show a line in the phase diagram for the nuclear matter liquid-gas phase transition.

One way to test the model and to compare its predictions with known observational data is to study the high density/low temperature part of the phase diagram

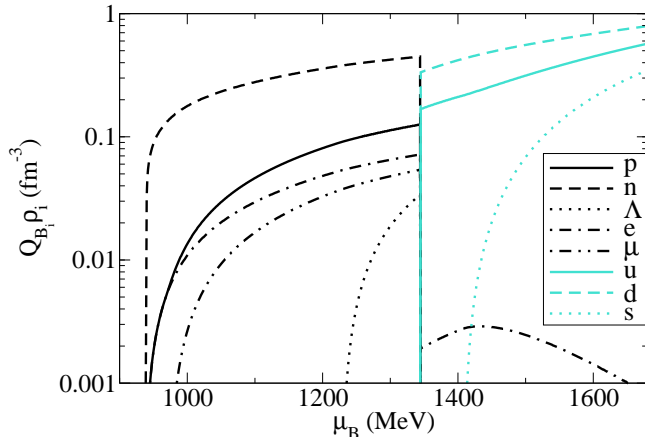


FIG. 4: (Color online) Population (baryonic density for different species as a function of baryonic chemical potential) for star matter at zero temperature using local charge neutrality

and compare our results with neutron star observations. The critical point for star matter lies at a slightly higher chemical potential than for the symmetric case and the first order transition line terminates on the zero temperature axis at $\mu_B = 1345$ MeV (grey line in Fig. 3). Up to this point, the charge neutrality was considered to be local, meaning that each phase had to be charge neutral by itself. At finite temperature the two phases contain mixtures of hadrons and quarks, which are dominated by hadrons or quarks, depending on the respective phase. At vanishing temperature there is no mixture, i.e. the system exhibits a purely hadronic and purely quark phase (Fig. 4). The density of electrons and muons is significant in the hadronic phase but not in the quark phase. The reason for this behavior is that because the down and strange quarks are also negatively charged, there is no necessity for the presence of electrons to generate charge neutrality, and only a small amount of leptons remains to assure beta equilibrium.

The quarks are totally suppressed in the hadronic phase and the hadrons are suppressed in the quark phase until a certain chemical potential (above 1700 MeV for $T = 0$). This behavior comes from the fact that the coupling constants in the Φ term of the effective mass formulas are high but still finite, so at very high chemical potential the threshold in Eq. (8) can be reached a second time for hadrons. This threshold, that is higher than the density in the center of neutron stars, establishes a limit for the applicability of the model. The hyperons, in spite of being included in the calculation, are suppressed by the appearance of the quark phase. Only a very small amount of Λ appears right before the phase transition (Fig. 4). The strange quarks appear after the other quarks and also do not make substantial changes in the system.

The possible neutron star masses and radii are cal-

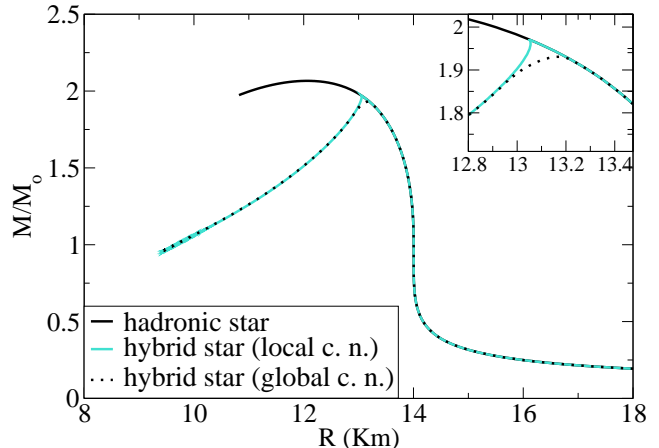


FIG. 5: (Color online) Mass-radius diagram

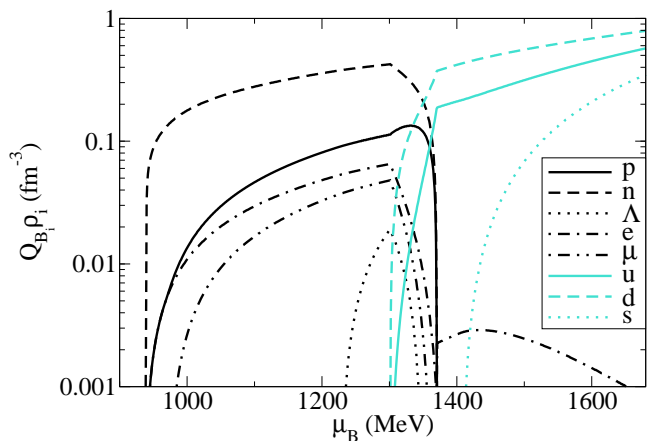


FIG. 6: (Color online) Population (baryonic density for different species as a function of baryonic chemical potential) for star matter at zero temperature using global charge neutrality.

culated solving the Tolmann-Oppenheimer-Volkof equations [18, 19]. The solutions for hadronic (same model but without quarks) and hybrid stars are shown in Fig. 5, where besides our equation of state for the core, a separate equation of state was used for the crust [20]. The maximum mass supported against gravity in our model is $2.1M_\odot$ in the first case and around $2.0M_\odot$ in the second. Because the equation of state for quark matter is much softer than the one for hadronic matter, the star becomes unstable right when the central density is higher than the phase transition threshold.

There is still another possible option for the configuration of the particles in the neutron star [21]. If instead of local we consider global charge neutrality, we find a

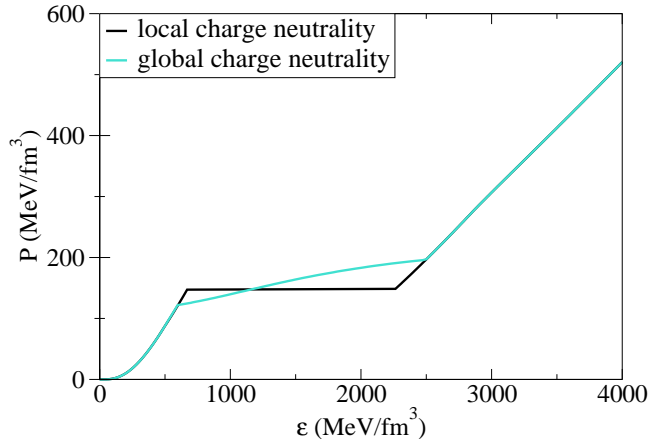


FIG. 7: (Color online) Equation of State (pressure as a function of energy density) for star matter at zero temperature using local and global charge neutrality.

mixture of phases. This possibility, which is a more realistic approach, changes the particle densities in the co-existence region making them appear and vanish in a smoother way (Fig. 6). Therefore, the maximum mass allowed for the star is slightly lower in this case than in the previous one, as can be seen from the dotted line in Fig. 5; however, this possibility allows stable hybrid stars with a small amount of quarks. The mixed phase

constitutes the inner core of the star up to a radius of approximately 2km. The equation of state for both cases is shown in Fig. 7. The large jump in the pressure in the local charge neutrality case explains why the neutron stars become immediately unstable after the phase transition in this configuration.

We conclude that our model is suitable for the description of neutron stars. The maximum mass predicted is around the most massive pulsars observed [22–26]. The radii lie in the allowed range being practically the same for hadronic or hybrid stars. A major advantage of our work compared to other studies of hybrid stars is that because we have only one equation of state for different degrees of freedom we can study in detail the way in which chiral symmetry is restored and the way deconfinement occurs at high temperature/density. Since the properties of the physical system, e.g. the density of particles in each phase, are directly connected to the order parameter for deconfinement Φ it is not surprising that we obtain different results in a combined description of the degrees of freedom compared to a simple matching of two separate equations of state.

Since the model additionally shows a realistic structure of the phase transition over the whole range of chemical potentials and temperatures as well as phenomenologically acceptable results for saturated nuclear matter, this approach presents an ideal tool for the study of ultrarelativistic heavy-ion collisions. Calculations along this line are in progress [27].

-
- [1] N. K. Glendenning, F. Weber and S. A. Moszkowski, *Phys. Rev. C* **45**, 844 (1992).
 - [2] F. Weber and M. K. Weigel, *Nucl. Phys. A* **505**, 779 (1989).
 - [3] J. Schaffner and I. N. Mishustin, *Phys. Rev. C* **53**, 1416 (1996) [arXiv:nucl-th/9506011].
 - [4] P. Papazoglou, D. Zschesche, S. Schramm, J. Schaffner-Bielich, H. Stoecker and W. Greiner, *Phys. Rev. C* **59**, 411 (1999).
 - [5] E. K. Heide, S. Rudaz and P. J. Ellis, *Nucl. Phys. A* **571**, 713 (1994) [arXiv:nucl-th/9308002].
 - [6] G. W. Carter, P. J. Ellis and S. Rudaz, *Nucl. Phys. A* **603**, 367 (1996) [Erratum-ibid. A **608**, 514 (1996)] [arXiv:nucl-th/9512033].
 - [7] L. Bonanno and A. Drago, arXiv:0805.4188 [nucl-th].
 - [8] F. Weber, *Prog. Part. and Nucl. Phys.* **54**, 193 (2005), and references therein.
 - [9] M. Buballa, *Phys. Rept.* **407**, 205 (2005) [arXiv:hep-ph/0402234].
 - [10] H. Heiselberg, C. J. Pethick and E. F. Staubo, *Phys. Rev. Lett.* **70**, 1355 (1993).
 - [11] K. Fukushima, *Phys. Lett. B* **591**, 277 (2004) [arXiv:hep-ph/0310121].
 - [12] P. Papazoglou, S. Schramm, J. Schaffner-Bielich, H. Stoecker and W. Greiner, *Phys. Rev. C* **57**, 2576 (1998).
 - [13] V. Dexheimer and S. Schramm, *Astrophys. J.* **683**, 943 (2008).
 - [14] J.D. Walecka, *Theoretical Nuclear And Subnuclear Physics* World Scientific Publishing Company; 2nd edition (2004).
 - [15] C. Ratti, M. A. Thaler and W. Weise, *Phys. Rev. D* **73**, 014019 (2006)
 - [16] S. Rosner, C. Ratti and W. Weise, *Phys. Rev. D* **75**, 034007 (2007)
 - [17] Z. Fodor and S. D. Katz, *JHEP* **0404**, 050 (2004) [arXiv:hep-lat/0402006].
 - [18] R. C. Tolman, *Phys. Rev.* **55**, 364 (1939).
 - [19] J. R. Oppenheimer and G. M. Volkoff, *Phys. Rev.* **55**, 374 (1939).
 - [20] G. Baym, C. Pethick and P. Sutherland, *Astrophys. J.* **170**, 299 (1971).
 - [21] N. K. Glendenning, *Phys. Rev. D* **46**, 1274 (1992).
 - [22] D. Barret, J. F. Olive and M. C. Miller, *Mon. Not. Roy. Astron. Soc.* **361**, 855 (2005) [arXiv:astro-ph/0505402].
 - [23] F. Ozel, *Nature* **441**, 1115 (2006).
 - [24] D. J. Champion *et al.*, arXiv:0805.2396 [astro-ph].
 - [25] J. Casares, J. I. G. Hernandez, G. Israelian and R. Rebolo, arXiv:0910.4496 [astro-ph.GA].
 - [26] T. Guver, F. Ozel, A. Cabrera-Lavers and P. Wroblewski, arXiv:0811.3979 [astro-ph].
 - [27] J. Steinheimer, V. Dexheimer, H. Petersen, M. Bleicher, S. Schramm and H. Stoecker, arXiv:0905.3099 [hep-ph].